Bcl-2 is necessary to counteract Bim and promote survival of TCRαβ+ CD8αα+ IEL precursors in the thymus

Sharmila Shanmuganad[1], **Sarah A. Hummel**[2], **Vivian Varghese**[2], **David A. Hildeman**[1,2,*]

[1]Immunology Graduate Program, Cincinnati Children's Hospital Medical Center and the University of Cincinnati College of Medicine, Cincinnati, OH 45229, USA

[2]Division of Immunobiology, Cincinnati Children's Hospital Medical Center and the University of Cincinnati College of Medicine, Cincinnati, OH 45229, USA

Abstract

The precursors of TCRαβ+ CD8αα+ intraepithelial lymphocytes (IEL) arise in the thymus through a complex process of agonist selection. We and others have shown that the pro-apoptotic protein, Bim, is critical to limit the number of thymic IEL precursors (IELp), as loss of Bim at the CD4+ CD8+ double positive (DP) stage of development drastically increases IELp. The factors determining this cell death versus survival decision remain largely unknown. Here, we used CD4CreBcl2$^{f/f}$ mice to define the role of the anti-apoptotic protein, Bcl-2, and CD4CreBcl2$^{f/f}$Bim$^{f/f}$ mice to determine the role of Bcl-2 in opposing Bim to promote survival of IELp. First, in wild-type mice, we defined distinct sub-populations within PD-1+ CD122+ IELp, based on their expression of Runx3 and α4β7. Co-expression of α4β7 and Runx3 marked IELp that were most dependent upon Bcl-2 for survival. Importantly, the additional loss of Bim restored Runx3+ α4β7+ IELp showing that Bcl-2 antagonizes Bim to enable IELp survival. Further, the loss of thymic IELp in CD4CreBcl2$^{f/f}$ mice also led to a dramatic loss of IEL in the gut and the additional loss of Bim restored gut IEL. The loss of gut IEL was due to both reduced seeding by IELp from the thymus as well as a requirement for Bcl-2 for peripheral IEL survival. Together, these findings highlight subset-specific and temporal roles for Bcl-2 in driving the survival of TCRαβ+ CD8αα+ IEL and thymic IELp.

Keywords

IEL precursors; thymic selection; Bcl-2; Bim; apoptosis; Runx3

Introduction

Intraepithelial lymphocytes are a heterogeneous population of immune cells important for regulating intestinal homeostasis (1–4). Recent studies also revealed the impact of IEL[2]

Corresponding Author: David A. Hildeman, Department of Pediatrics, Division of Immunobiology, MLC 7038, Cincinnati Children's Hospital Medical Center, 3333 Burnet Avenue, Cincinnati, OH 45229. , David.Hildeman@cchmc.org, Phone: 513-636-3923, Fax: 513-636-5355.

on metabolism and cardiovascular health (5). IEL are broadly classified into natural and induced IEL. Induced IEL comprise of TCRαβ+CD4+ and TCRαβ+CD8αβ+ IEL that arise from peripheral T cells. Natural IEL include TCRαβ+ and TCRγδ+ IEL that don't express the classical co-receptors, but instead express the CD8αα homodimer and arise from precursor cells that differentiate in the thymus (6–8)

During development, CD4 and CD8 single positive thymocytes go through the process of positive and negative selection that generate CD4+ and CD8+ T cells with diverse T cell receptor repertoires. Other cells, including NKT[3] cells, Treg[4] and precursors of TCRαβ+ CD8αα+ IEL undergo an ill-defined process of thymic agonist selection, an alternative cell fate associated with strong TCR signals (9–12). Recent data show that the repertoire of IELp[5] is controlled after β-selection and before classical positive selection (13), likely by pre-TCR signal strength (14). In addition to this early repertoire selection step, most IELp also progress through a CD4+ CD8+ DP[6] stage as shown by fate mapping mice (15). Developmentally, a subset of DP cells expressing CD8αα (CD4+ CD8αβ + CD8αα + triple positive (TP)[7] cells) and very little TCRβ and CD5 are the earliest identified pre-selection IELp to date (16). IELp are thought to further progress when DP cells recognize self-ligands with high affinity TCR interactions, downregulate CD4 and CD8 and upregulate markers of high TCR signaling, like PD-1[8], to become part of the post-selected (TCRβ+ CD5+) , CD4- CD8− double negative(DN[9]) thymocyte pool (9, 16–20). Within these post-selected DN cells, those expressing CD122, a marker of self-reactive, mature cells (21, 22), have the strongest propensity to populate the small intestine and become TCRαβ+ CD8αα+ IEL (22, 23). Recent studies examining IELp heterogeneity identified CD122+ subsets based on their expression of PD-1 and Tbet that vary in MHC restriction, TCR usage, emigration, integrin expression (22–25) and timing of gut seeding (26). While progress has been made in characterizing thymic IELp subsets, the factors that control their survival are just beginning to be elucidated.

Apoptosis plays a crucial role in cell fate and survival decisions in the thymus and is initiated by the interpretation of TCR signals by pro and anti-apoptotic proteins of the Bcl-2 family that physically interact to regulate cytochrome c release from the mitochondria (27, 28). Bim plays a critical role in thymic development, controlling negative selection (29) as well as IELp development (20, 22, 30) . While we previously showed that Bcl-2 plays a critical role in opposing Bim to promote memory CD8+ T cell survival (31–33), the factors that antagonize Bim to promote IELp survival remain unclear. Indeed, despite the normal presence of Bim, it remains unclear how some IELp survive. While transgenic overexpression of pro-survival Bcl-2 family proteins resulted in increased thymic IELp and TCRαβ+ CD8αα+ IEL, similar to the loss of Bim, these studies did not examine the natural

[2]IEL Intraepithelial lymphocyte
[3]NKT Natural killer T cell
[4]Treg T regulatory cell
[5]IELp Intraepithelial lymphocyte precursor
[6]DP Double positive
[7]TP triple positive
[8]PD-1 programmed cell death=1
[9]DN Double negative

antagonists of Bim that control IELp survival (20, 34–36). Thus, the role of Bcl-2 as a critical Bim antagonist in thymic IELp remains to be rigorously tested.

To avoid substantial issues in global Bcl-2-deficient mice (37), we used CD4CreBcl2$^{f/f}$ mice, in which Bcl-2 was selectively deleted at the DN to DP transition, and found a marked reduction in a subset of post-selected DN thymocytes that express PD-1 and CD122. Further, within PD-1+ CD122+ thymocytes, we identified a population that had recently experienced TCR signals and a more mature population, expressing Runx3 and enriched for markers of IELp, which critically depended on Bcl-2 to combat Bim for survival. Bcl-2 mediated IELp survival was independent of IL-2 and IL-15 cytokine signals. Importantly, in addition to its role in thymic IELp survival, we also found that Bcl-2 was critical for peripheral survival of gut IEL, and both roles contributed to an almost complete lack of TCRαβ+ CD8αα+ IEL in the gut. Thus, while the loss of Bcl-2 was imperceptible at the whole DN population, a small sub-population of IELp thymocytes was drastically reduced, which contributed to the dramatic loss of TCRαβ+ CD8αα+ IEL in CD4CreBcl2$^{f/f}$ mice.

Materials and methods:

Mice

C57BL/6 mice were purchased from Taconic Farms. Bcl2$^{f/f}$ mice were a gift from Dr.Ira Tabas (Columbia University, New York) and were crossed to CD4Cre^{+} mice obtained from The Jackson Laboratory. Bim$^{f/f}$ mice were generated in collaboration with Dr. Philippe Bouillet (38, 39) and crossed to CD4Cre^{+} mice obtained from The Jackson Laboratory. Nur77^{GFP} mice (C57BL/6-Tg (Nr4a1-EGFP/cre) 820Khog/J) were obtained from The Jackson Laboratory. CD4CreBcl2$^{f/f}$ mice were crossed to CD4CreBim$^{f/f}$ mice. Mice for the thymus studies were between 3-5 weeks of age and for the gut studies between 5-8 weeks of age. Experimental and control mice were littermates in most cases and both male and female mice were used. Wild-type (WT)[10] mice mentioned in figure legends are C57BL/6, Bcl2$^{f/f}$, Bim$^{f/f}$ or Bcl2f$^{/f}$ Bim$^{f/f}$ mice, we have not observed significant differences in any of these lines of mice. Animals were housed under specific-pathogen-free conditions in the Division of Veterinary Services (Cincinnati Children's Hospital Medical Center, Cincinnati, OH), and experimental procedures were reviewed and approved by the Institutional Animal Care and Use Committee at the Cincinnati Children's Hospital Research Foundation.

Cell processes and flow cytometry

Thymi or spleens from individual mice were harvested and crushed through a 100μm mesh strainer and red blood cells were lysed to generate single-cell suspensions. IEL isolation was performed by following a modified protocol (40). Briefly, the small intestine was cut off and washed with $Ca^{2+}Mg^{2+}$-free HBSS for removing feces and mucus. After removing Peyer's patches, the small intestine was cut in pieces and shaken in $Ca^{2+}Mg^{2+}$-free HBSS supplemented with 5% FBS, 2 mM EDTA, and 1 mM DTT (Sigma-Aldrich), twice , for 15 min at 37°C. The IEL in the supernatant were purified with Percoll (GE Healthcare) gradient .The single-cell suspension was further analyzed by flow cytometry

[10]WT wild type

after excluding dead cells by using the Live Dead staining kit (Invitrogen). 2-3 million cells were stained with tetramers that recognize CD1d (PBS-57) or Thymic Leukemia (TL) antigen (T3b) (NIH Tetramer Core Facility) followed by staining with antibodies against CD4, TCRβ, CD5, $α_4β_7$, Runx3 (BD Biosciences), CD25, CD8α, PD-1, CD122, CD44, CD45.2, CD8β, Bcl-2, Ki-67, TCRδ, CD49b, NKp46 (Biolegend), Bim (Cell Signaling) or Tbet, FoxP3 (Invitrogen). Intracellular stains were performed using the FoxP3/transcription factor staining buffer set (Invitrogen). For detection of Bim, secondary anti-rabbit IgG Ab was used (Invitrogen). The cells were acquired on a BD LSRFortessa flow cytometer and analyzed by FACSDiva software (BD Biosciences) or FlowJo software (FlowJo).

In vivo cytokine neutralization

Anti-IL-2 Ab (clones S4B6 and JES6-1A12) and rat IgG2a isotype control (2A3) were purchased from Bio X Cell. Anti-IL-15 (M96) was a kind gift from Amgen. For IL-2 and IL-15 neutralization, 3 week old mice were injected i.p with 150 μg of S4B6 and Jes61A12 and 25 μg of M96 or with 150 μg isotype control (2A3), on days 0, 2, 4 and 6.The mice were sacrificed on day 7 and thymii and spleen were harvested.

Statistical analysis

GraphPad Prism and Microsoft Excel software was used to analyze data and generate graphs. Statistical tests were performed as described in the figure legends.

Results

Bcl-2 contributes to the accrual of post-selected DN thymocytes

Given the role of Bim in limiting IELp survival (20, 30), we examined the role of a major Bim antagonist, Bcl-2, in promoting IELp survival. To temporally delete Bcl-2 during thymic development, we bred Bcl2$^{f/f}$ (41) mice to CD4Cre+ mice. First, overall numbers of pre-selection triple positive (TP− CD4+ CD8αβ + CD8αα) IELp were not affected by the loss of Bcl-2 (Fig 1A). Next, we assessed DN cells (CD4− CD8−) after excluding NKT cells (CD1d tetramer +) and potential Treg precursors (CD25+) (22) and did not see a significant loss of DN cell numbers in CD4CreBcl2$^{f/f}$ mice (Fig 1B). In contrast, the frequency and total numbers of post-selected DN cells (CD4− CD8− CD5+ TCRβ+) dropped significantly in CD4CreBcl2$^{f/f}$ mice compared to wild-type (WT) mice (Fig 1B). This reliance on Bcl-2 was associated with higher Bcl-2 expression in CD5+ TCRβ+ DN cells compared to DP cells in WT mice (Fig 1C). Of note, the levels of Bim were significantly lower in CD5+ TCRβ+ DN cells in CD4CreBcl2$^{f/f}$ mice compared to WT mice (Fig 1C). Thus, post-selected DN thymocytes normally express higher levels of Bcl-2 that is required for their accumulation.

Bcl-2 is critical for the survival of CD122+ thymocytes that experience strong TCR signaling

IELp consist of multiple subpopulations, including self-reactive PD-1+ cells and non-self-reactive Tbet+ cells (22, 24). The frequencies and numbers of both PD-1+ and Tbet+ cells were significantly reduced in CD4CreBcl2$^{f/f}$ mice relative to WT mice (Fig 2A). Recent work showed that CD122 expression is associated with high affinity antigen encounter and

IELp potential (23), and that PD-1 upregulation precedes CD122 upregulation (42). Using these markers as a temporal guide, we found that ~ 45% of PD-1+ cells were CD122+ while nearly all Tbet+ cells were CD122+ (Fig 2B). Compared to WT mice, CD4CreBcl2[f/f] mice displayed a significant drop in frequency and a roughly 5-fold loss in the numbers of CD122+ cells in both PD-1+ and Tbet+ populations (Fig 2B). In contrast, Bcl-2 was not required to maintain normal numbers of CD122– cells in either the PD-1+ or Tbet+ populations. Again, consistent with their dependence upon Bcl-2, in WT mice we observed a 3-4-fold increase in Bcl-2 levels in PD-1+ cells that co-expressed CD122 (Fig 2C). The PD-1+ CD122+ cells that survived in CD4CreBcl2[f/f] mice had significantly lower levels of Bim in comparison to WT mice (Fig 2C). In contrast, Tbet+ cells did not have a significant difference in Bim levels between WT and CD4CreBcl2[f/f] mice. (Fig 2C).

Runx3 expression marks a sub-population of PD-1+ CD122+ thymocytes that are enriched for markers of IELp and are critically dependent on Bcl-2 for survival

The integrin α4β7 is upregulated on some PD-1+ CD122+ IELp and necessary for their ability to home and be retained in the gut (23, 43).Further, unlike Tbet+ IELp, no lineage-defining transcription factors have been identified for PD-1+ CD122+ IELp. As Runx3 is a critical driver of CD8α re-expression (44) and differentiation of IELp into TCRαβ+ CD8αα+ IEL (35), we explored the expression of Runx3 and α4β7 amongst PD1+ CD122+ thymocytes after excluding CD44^{hi} cells (~10%, Supplemental Fig 1A) as PD-1+ IELp are predominantly negative for CD44 expression (22). Interestingly, Runx3 appeared to be co-expressed with α4β7 in a subpopulation of PD-1+ CD122+ cells but not PD-1+ CD122– cells (Supplemental Fig 1B, Fig 3A). Roughly 30% of PD-1+ CD122+ cells expressed both Runx3 and α4β7, ~16% expressed Runx3 but not α4β7, and ~10% expressed α4β7 but not Runx3, while the rest (~44%) lacked expression of both markers (Fig 3A). Bcl-2 was required for normal numbers of all 4 subpopulations with Runx3+ α4β7+ cells being maximally impacted (~3 fold) (Fig 3A).

To further discern temporal information regarding these post-selected PD-1+ CD122+ sub-populations, we examined levels of CD69, a transient indicator of recent TCR stimulation. Runx3– α4β7– cells were predominantly CD69^{hi} while Runx3– α4β7+, Runx3+ α4β7–, and Runx3+ α4β7+ cells had low expression of CD69 (Fig 3B). Prior data indicates that CD122+ cells that are α4β7^{hi} and CD69^{lo} are temporally the most distant from the DP stage (22, 23), suggesting that Runx3+ α4β7+ cells are the most differentiated IELp subset and are poised to emigrate to the gut. Also, the levels of Bcl-2 were highest in Runx3+ α4β7+ cells, followed by Runx3+ α4β7– and Runx3– α4β7+ cells, while Runx3– α4β7– cells expressed Bcl-2 at similar levels to PD-1+ CD122– cells (Fig 3C). Runx3+ α4β7+ IELp also expressed moderate levels of CD5 and Nur77(measured in a Nur77[GFP]reporter mouse(45))and high CD122 in comparison to the least mature CD122+ IELp that lacked expression of both Runx3 and α4β7 (Supplemental Fig 2).

As common gamma-chain cytokine signaling induces Bcl-2 expression (46), we examined the role of IL-2/15 signaling on Bcl-2 levels and PD-1+ CD122+ IELp survival by neutralizing IL-2 and IL-15. The efficiency of neutralization was confirmed by assessing natural killer cell and Treg depletion in the spleen (Supplemental Fig 3A–B). IL-2/15

neutralization did not impact Bcl-2 levels (Supplemental Fig 3C) and a small proportion of Runx3+ α4β7+ IELp showed reduced proliferation, but their overall numbers were not reduced (Supplemental Fig 3D). Combined, these data show that Bcl-2 is critical for the survival of CD122+ cells, particularly Runx3+ α4β7+ IELp, in an IL-2 and IL-15 independent manner.

Bim culls both CD122+ and CD122– thymocytes with the most impact on PD-1+ CD122+ α4β7+ thymocytes

One function of Bcl-2 is physical sequestration and antagonization of Bim (28, 47). Interestingly, and similar to Bcl-2, Bim levels appeared highest within Runx3+ α4β7+ IELp, slightly lower in Runx3– α4β7+ and Runx3+ α4β7– cells and even lower in Runx3– α4β7– cells (Fig 3C). Using CD4CreBim^f/f mice we found that the loss of Bim massively increased the accumulation of CD5+ TCRβ+ DN and PD-1+ thymocytes (Fig 4A), but not as much Tbet+ IELp, consistent with prior work (22). Further, loss of Bim led to a significant accrual of CD122+ cells (~35 fold) and to a lesser extent CD122– cells (~8 fold) among the PD-1+ population compared to WT (Fig 4A). We also found that Bim was required to limit the numbers of all four PD-1+ CD122+ sub-populations that also required Bcl-2, and the greatest effect was in Runx3– α4β7+ cells (Fig 4B) with ~290 fold increase compared to WT. Runx3+ α4β7+ IELp were also substantially increased (~180 fold) in the absence of Bim, but despite their increased numbers, they had reduced Runx3 levels (Fig 4C). Further, these Runx3+α4β7+ cells had very low levels of Bcl-2 suggesting that the absence of Bim allowed visualization of cells that otherwise would have perished (Fig 4D). Similarly, the loss of Bcl-2 also led to reduced Runx3 levels (Fig 4C). Taken together, these data show that Bim is required for the clonal deletion of CD122+ IELp encountering strong TCR stimulation and limits their differentiation into Runx3 and α4β7 expressing cells.

Additional loss of Bim rescues PD-1+ CD122+ thymocytes in Bcl-2 deficient mice

Consistent with Bcl-2 as a critical antagonist of Bim, the additional loss of Bim largely restored CD5+ TCRβ+ DN and PD-1+ cells that lacked Bcl-2 (Fig 4A). In contrast, Tbet+ cells that were decreased in CD4CreBcl2^f/f mice were only partially restored in CD4CreBim^f/fBcl2^f/f mice. Further, though CD122– and CD122+ cells within the PD-1+ population were increased above WT levels, CD122+ cells were not rescued to the levels seen in CD4CreBim^f/f mice. (Fig 4A). Among the CD122+ subpopulations, Runx3– α4β7+ cells and Runx3+ α4β7+ IELp showed a similar pattern of rescue above WT, but not to the extent observed in the absence of Bim alone (Fig 4B). Notably, we confirmed that Bim and Bcl-2 were predominantly deleted in all these populations (Supplemental Fig 4A). Examination of other Bcl-2 family members in CD122+ cells revealed a difference in the levels of anti-apoptotic Mcl-1 and pro-apoptotic Noxa between CD4CreBim^f/f mice and CD4CreBim^f/fBcl2^f/f mice (Supplemental Fig 4B). Taken together, our data show that Bcl-2 is critical to counteract the pro-apoptotic activity of Bim to control the homeostasis of PD-1+ CD122+ thymocytes.

Thymic expression of Bcl-2 is critical for the survival of TCRαβ+ CD8αα+ IEL and loss of Bim rescues their survival

Given the requirement of Bcl-2 in thymic development of IELp, we examined whether this translated to TCRαβ+ CD8αα+ IEL in the gut. 8 week old CD4CreBcl2$^{f/f}$ mice showed a striking loss (~30 fold) of TCRαβ+ CD8αα+ IEL, whereas TCRαβ+ CD8αβ+ IEL showed around a 5-fold reduction (Fig 5A). Interestingly, even as early as 5 weeks, we found that the few remaining TCRαβ+ CD8αα+ IEL in CD4CreBcl2$^{f/f}$ mice had not deleted Bcl-2 despite relatively efficient deletion (~90%) in thymic IELp as well as in TCRαβ+ CD8αβ+ IEL in the gut (Fig 5B , middle row). As the initial seeding of the gut by thymic IELp occurs between 2-3 weeks of age, we examined Bcl-2 expression in IEL in 3 week old mice. In contrast to 5 week old mice, 3 week old CD4CreBcl2$^{f/f}$ mice showed >90% Bcl-2 deletion in TCRαβ+ CD8αα+ IEL (Fig 5B, top row). Importantly, the numbers of TCRαβ+ CD8αα+ IEL in 3 week old CD4CreBcl2$^{f/f}$ mice were significantly decreased, consistent with substantially reduced seeding from the thymus (Fig 5C). We assessed Ki-67 expression and found no drop in proliferation, excluding impaired proliferation as a mechanism for the reduced numbers (Fig 5D).Strikingly, we found that the additional loss of Bim completely restored Bcl-2-deleted cells at 5 weeks of age (Fig 5B, bottom row), highlighting the role of Bim in driving the selection of Bcl-2^{hi} cells and correspondingly, the number of TCRαβ+ CD8αα+ IEL were rescued (Fig 5C). Combined, these data show that both thymic and peripheral Bcl-2 expression critically affects gut IEL survival by combating Bim.

Discussion

Here we identified Bcl-2 as a critical antagonist of Bim in the thymic precursors of TCRαβ+ CD8αα+ IEL. The gain and loss of cells in mice deficient in Bcl-2 and/or Bim was instructive in our understanding of thymic CD122+ IELp development. Combined with the expression of maturation markers, our data are consistent with a scenario in which Runx3− α4β7− cells are the least mature, PD-1+ CD122+ thymocytes having just undergone TCR signaling as they are CD69^{hi} and Nur77^{hi}(45) and minimally affected by the loss of Bcl-2. Runx3− α4β7+ and Runx3+ α4β7+ cells are more mature as they have lower levels of CD69 and Nur77 and higher levels of α4β7 and are most affected by the loss of Bcl-2. Notably, Runx3+ α4β7+ IELp match the phenotype of an 'agonist-selected' cluster recently identified in a thymic single-cell transcriptomic analysis in their expression of Runx3, moderate levels of CD5 and Nur77, high CD122 and low CD69, suggesting that they represent the most mature , agonist-selected, thymic IELp (48).

While we showed that IL-2/15 signaling wasn't required for Bcl-2 expression in Runx3+ α4β7+ IELp, we think that TCR signals likely contribute to their survival. One scenario for high Bcl-2 acquisition in a subset of CD122+ cells is through pathways specific to agonist signals. For example, mice deficient in RasGRP1 and α- chain connecting peptide domain (α-CPM) have impaired agonist selection (9, 23) . Notably, Stim1/Stim2-deficient mice have impaired agonist selection (49) and reduced acquisition of the TCRβ^{hi} DP^{lo} PD-1^{hi} phenotype (18). The Stim1/Stim2 pathway involving store-operated calcium, triggered upon high affinity TCR signals, induces transcription factors like Egr2 (49) known to induce Bcl-2 (50). Furthermore, Stim1/Stim2-deficient mice displayed reduced post-selected DN numbers

and CD122 levels (49). Although the authors attributed this loss to reduced proliferation due to impaired cytokine signaling through CD122, we showed that very few PD-1+ CD122+ IELp proliferated in an IL-2/15 dependent manner, and their numbers remain unaffected upon IL-2/IL-15 neutralization in agreement with prior studies (22, 51). Thus, our data is consistent with a model in which TCR signaling primarily upregulates Bcl-2. However, this does not rule out a potential role for Bcl-2 at an earlier stage of IELp development - shortly after beta-selection via signals emanating from the pre-TCR (13, 14, 52). Moreover, recent data point to a potential role for TGF-β in maintaining Bcl-2 expression in post-selected DN thymocytes (53). Finally, it is also possible that high Bcl-2 levels may be due to escape from B7 signaling as CD28 signaling can reduce Bcl-2 *in vitro* (54) and B7 KO mice have impaired clonal deletion of post-selected DN (35). It would be interesting to determine whether B7 signals contribute to Bim and Bcl-2 expression in IELp and if Bcl-2 is required for the increased IELp found in B7-deficient animals.

While Bim kills PD-1+ CD122− cells, whose DP^{lo} and PD-1^{hi} phenotype may be indicative of cells undergoing negative selection (20), its effects were most apparent in PD-1+ CD122+ cells which experience the highest TCR signaling and are associated with IELp agonist selection (23). Prior work has shown that TCR signaling is known to increase Bim levels (29). Our data demonstrate that the only PD-1+ CD122+ thymocytes that survive in the presence of Bim are those with high levels of Bcl-2 that enable them to antagonize Bim-mediated death. Indeed, in the absence of Bim, we observed Bcl2^{lo} cells, while in the absence of Bcl-2, Bim^{lo} cells emerged. These data show that the levels of Bim and Bcl-2 are tightly aligned and are critical controllers of PD-1+ CD122+ IELp survival. However, additional Bcl-2 family members may also play a role in CD122+ IELp homeostasis. For example, the decrease in PD-1+ CD122+ cells in CD4CreBcl2$^{f/f}$Bim$^{f/f}$ mice relative to CD4CreBim$^{f/f}$ mice suggests that Bcl-2 antagonizes pro-apoptotic molecules other than Bim(55–57).We examined the levels of pro-apoptotic molecules and found that Noxa levels were significantly lower in PD-1+ CD122+ cells in the absence of Bcl-2 (Supplementary Fig 4B), suggesting Noxa as a potential Bcl-2 antagonist. However, it may be a little more complex than involvement of a single pro-apoptotic family member as we found that the levels of anti-apoptotic molecule Mcl-1 were also increased in PD-1+ CD122+ cells in CD4CreBcl2$^{f/f}$ mice (Supplementary Fig 4B). We wish to stipulate that these results reflect cells that may have undergone adaptation to the lack of Bim and must be interpreted with that caveat when thinking about roles for additional Bcl-2 family member involvement. Nonetheless, while Bim and Bcl-2 play dominant roles in PD-1+CD122+ IELp, more work is required determine the potential roles of additional Bcl-2 family members and their contribution to thymic IELp homeostasis.

While our data clearly show that the absence of Bim increases the numbers of PD-1+ CD122+ sub-populations that we have defined on the basis of Runx3 and α4β7 expression, the relationship between these sub-populations in the context of IELp differentiation remain unclear. Further work will define the temporal relationships between these sub-populations and their sensitivity to Bim-mediated death. Based on the fact that the levels of Runx3 are lower in Runx3+ α4β7+ IELp in the absence of Bim, we hypothesize that the absence of Bim promotes their survival, but may not completely restore differentiation.

Moreover, CD4CreBim**f/f** mice, have a much lower gut increase in TCRαβ+ CD8αα+ IEL (~8 fold) relative to the increase in Runx3+ α4β7+ thymic IELp (~180 fold). One explanation for this could be a reduction in migration and/or survival of IELp as they traffic to the gut. Indeed, on examining the spleen, through which IELp traffic before populating the gut (20, 30), the increase in splenic IELp in CD4CreBim**f/f** mice was closer to the increase observed in the gut (~ 13 fold, Supplemental Fig 3E). It is also possible that in the absence of Bim, IEL differentiation is impaired when IELp seed the gut, given that IELp in CD4CreBim**f/f** mice have significantly lower Runx3 levels and Runx3 is critical for TCRβ+ CD8αα+ IEL differentiation (35). Similarly, CD4CreBcl2$^{f/f}$ mice also have low levels of Runx3 in Runx3+ α4β7+ IELp and this likely leads to impaired IEL maturation, which may explain the higher ~ 30-40 fold loss of gut TCRβ+ CD8αα+ IEL compared to ~5.5 fold loss of thymic IELp. In further support, transgenic expression of Bcl-2 was unable to rescue IEL deficiency in Runx3-deficient mice (35), consistent with an uncoupling of survival from differentiation. However, the role of Bcl-2 in peripheral survival of TCRαβ+ CD8αα+ IEL (evidenced by a temporal selection for Bcl-2^{hi} cells) also contributes to their profound loss in the gut.

While the importance of Runx3 in the final maturation of IEL in the gut is known (16, 24, 35, 58), our results show that Runx3 expression is actually established in a small subpopulation of CD122+ thymic IELp. This might explain why other groups found that total TCRβ+ DN thymocytes were unchanged in Runx3 deficient mice (35). Similarly, we saw that total numbers of DN cells were not affected in Bcl-2-deficient mice, but a small Runx3+ α4β7+ subset was dramatically decreased. Thus, the role of Runx3 in the thymic IELp fate decision needs to be re-examined in light of our work. The signals driving thymic Runx3 expression are yet unknown. Unlike in CD8+ thymocytes, where common gamma-chain cytokines play a role in Runx3 induction, we ruled out IL-2/15 mediated Runx3 upregulation in Runx3+ α4β7 + IELp as their blockade did not affect Runx3 expression (data not shown). Further, IELp do not express the IL-7Rα chain (35) precluding a role for IL-7 mediated Runx3 induction.

While prior studies used transgenic overexpression of anti-apoptotic proteins, our temporally relevant deletion model overcomes the caveats of non-physiological expression of Bcl-2 family members and potential skewing of interacting partners and reveals Bcl-2 as the critical Bim antagonist involved in both thymic IELp and TCRαβ+ CD8αα+ IEL survival. We previously showed that Bim affects the TCR repertoire of post-selected DN cells in the periphery (30) and while TCR self-reactivity was conserved in Bcl-2 transgenic mice (34, 59), the effect of loss of Bcl-2 on the TCR repertoire of IELp and IEL require further study. As prior work associated Bim with inflammatory bowel disease (60), one possible role for Bim (and Bcl-2) is to hone the TCR repertoire of IEL that are critical for regulation of gut injury. As mentioned earlier, repertoire selection may occur prior to classical positive selection (13) and experiments are underway to determine the impact of temporal deletion of Bim and Bcl-2 on thymic IELp repertoires. Nonetheless, as TCRαβ+ CD8αα+ IEL have a cytotoxic phenotype, it will be important to test if TCR repertoire changes of IEL impact defense against gut pathogens. Due to the virtual absence of TCRαβ+ CD8αα+ IEL in the gut of CD4CreBcl2$^{f/f}$ mice, we think they can be a useful tool to interrogate the role of these cells *in vivo*, with the caveat that the absence of Bcl-2 modestly reduces

conventional CD4+ and CD8+ T cells. Nonetheless, the role of TCRαβ+ CD8αα+ IEL in phenotypes uncovered in CD4CreBcl2$^{f/f}$ mice would need to be validated via adoptive transfer of TCRαβ+ CD8αα+ IEL from wildtype mice back into these mice and assessing their contribution to gut homeostasis.

Supplementary Material

Refer to Web version on PubMed Central for supplementary material.

Acknowledgments

References

1. Cheroutre H, Lambolez F, and Mucida D. 2011. The light and dark sides of intestinal intraepithelial lymphocytes. Nat Rev Immunol 11: 445–456. [PubMed: 21681197]

2. McDonald BD, Jabri B, and Bendelac A. 2018. Diverse developmental pathways of intestinal intraepithelial lymphocytes. Nat Rev Immunol 18: 514–525. [PubMed: 29717233]

3. Hoytema van Konijnenburg DP, Reis BS, Pedicord VA, Farache J, Victora GD, and Mucida D. 2017. Intestinal Epithelial and Intraepithelial T Cell Crosstalk Mediates a Dynamic Response to Infection. Cell 171: 783–794 e713. [PubMed: 28942917]

4. Sujino T, London M, Hoytema van Konijnenburg DP, Rendon T, Buch T, Silva HM, Lafaille JJ, Reis BS, and Mucida D. 2016. Tissue adaptation of regulatory and intraepithelial CD4(+) T cells controls gut inflammation. Science 352: 1581–1586. [PubMed: 27256884]

5. He S, Kahles F, Rattik S, Nairz M, McAlpine CS, Anzai A, Selgrade D, Fenn AM, Chan CT, Mindur JE, Valet C, Poller WC, Halle L, Rotllan N, Iwamoto Y, Wojtkiewicz GR, Weissleder R, Libby P, Fernandez-Hernando C, Drucker DJ, Nahrendorf M, and Swirski FK. 2019. Gut intraepithelial T cells calibrate metabolism and accelerate cardiovascular disease. Nature 566: 115–119. [PubMed: 30700910]

6. Guy-Grand D, and Vassalli P. 2002. Gut intraepithelial lymphocyte development. Curr Opin Immunol 14: 255–259. [PubMed: 11869901]

7. Guy-Grand D, Azogui O, Celli S, Darche S, Nussenzweig MC, Kourilsky P, and Vassalli P. 2003. Extrathymic T cell lymphopoiesis: ontogeny and contribution to gut intraepithelial lymphocytes in athymic and euthymic mice. J Exp Med 197: 333–341. [PubMed: 12566417]

8. Lambolez F, Kronenberg M, and Cheroutre H. 2007. Thymic differentiation of TCR alpha beta(+) CD8 alpha alpha(+) IELs. Immunol Rev 215: 178–188. [PubMed: 17291288]

9. Leishman AJ, Gapin L, Capone M, Palmer E, MacDonald HR, Kronenberg M, and Cheroutre H. 2002. Precursors of functional MHC class I- or class II-restricted CD8alphaalpha(+) T cells are positively selected in the thymus by agonist self-peptides. Immunity 16: 355–364. [PubMed: 11911821]

10. Baldwin TA, Hogquist KA, and Jameson SC. 2004. The fourth way? Harnessing aggressive tendencies in the thymus. J Immunol 173: 6515–6520. [PubMed: 15557139]

11. Stritesky GL, Jameson SC, and Hogquist KA. 2012. Selection of self-reactive T cells in the thymus. Annu Rev Immunol 30: 95–114. [PubMed: 22149933]

12. Ruscher R, and Hogquist KA. 2019. Development, ontogeny, and maintenance of TCRalphabeta(+) CD8alphaalpha IEL. Curr Opin Immunol 58: 83–88. [PubMed: 31146182]

13. Verstichel G, Vermijlen D, Martens L, Goetgeluk G, Brouwer M, Thiault N, Van Caeneghem Y, De Munter S, Weening K, Bonte S, Leclercq G, Taghon T, Kerre T, Saeys Y, Van Dorpe J, Cheroutre

H, and Vandekerckhove B. 2017. The checkpoint for agonist selection precedes conventional selection in human thymus. Sci Immunol 2.

14. Grandjean CL, Sumaria N, Martin S, and Pennington DJ. 2017. Increased TCR signal strength in DN thymocytes promotes development of gut TCRalphabeta((+))CD8alphaalpha((+)) intraepithelial lymphocytes. Sci Rep 7: 10659. [PubMed: 28878277]

15. Eberl G, and Littman DR. 2004. Thymic origin of intestinal alphabeta T cells revealed by fate mapping of RORgammat+ cells. Science 305: 248–251. [PubMed: 15247480]

16. Gangadharan D, Lambolez F, Attinger A, Wang-Zhu Y, Sullivan BA, and Cheroutre H. 2006. Identification of pre- and postselection TCRalphabeta+ intraepithelial lymphocyte precursors in the thymus. Immunity 25: 631–641. [PubMed: 17045820]

17. McGargill MA, and Hogquist KA. 1999. Antigen-induced coreceptor down-regulation on thymocytes is not a result of apoptosis. J Immunol 162: 1237–1245. [PubMed: 9973375]

18. McDonald BD, Bunker JJ, Erickson SA, Oh-Hora M, and Bendelac A. 2015. Crossreactive alphabeta T Cell Receptors Are the Predominant Targets of Thymocyte Negative Selection. Immunity 43: 859–869. [PubMed: 26522985]

19. Yamagata T, Mathis D, and Benoist C. 2004. Self-reactivity in thymic double-positive cells commits cells to a CD8 alpha alpha lineage with characteristics of innate immune cells. Nat Immunol 5: 597–605. [PubMed: 15133507]

20. McDonald BD, Bunker JJ, Ishizuka IE, Jabri B, and Bendelac A. 2014. Elevated T cell receptor signaling identifies a thymic precursor to the TCRalphabeta(+)CD4(−)CD8beta(−) intraepithelial lymphocyte lineage. Immunity 41: 219–229. [PubMed: 25131532]

21. Nakase K, Kita K, Anazawa H, Hoshino K, Shirakawa S, Tanaka I, and Tsudo M. 1994. Induction of interleukin-2 receptor alpha chain expression of immature acute myelocytic leukemia cells. Leuk Res 18: 269–274. [PubMed: 7513371]

22. Ruscher R, Kummer RL, Lee YJ, Jameson SC, and Hogquist KA. 2017. CD8alphaalpha intraepithelial lymphocytes arise from two main thymic precursors. Nat Immunol 18: 771–779. [PubMed: 28530714]

23. Golec DP, Hoeppli RE, Henao Caviedes LM, McCann J, Levings MK, and Baldwin TA. 2017. Thymic progenitors of TCRalphabeta(+) CD8alphaalpha intestinal intraepithelial lymphocytes require RasGRP1 for development. J Exp Med 214: 2421–2435. [PubMed: 28652304]

24. Klose CS, Blatz K, d'Hargues Y, Hernandez PP, Kofoed-Nielsen M, Ripka JF, Ebert K, Arnold SJ, Diefenbach A, Palmer E, and Tanriver Y. 2014. The transcription factor T-bet is induced by IL-15 and thymic agonist selection and controls CD8alphaalpha(+) intraepithelial lymphocyte development. Immunity 41: 230–243. [PubMed: 25148024]

25. Klose CSN, Hummel JF, Faller L, d'Hargues Y, Ebert K, and Tanriver Y. 2018. A committed postselection precursor to natural TCRalphabeta(+) intraepithelial lymphocytes. Mucosal Immunol 11: 333–344. [PubMed: 28745324]

26. Ruscher R, Lee ST, Salgado OC, Breed ER, Osum SH, and Hogquist KA. 2020. Intestinal CD8alphaalpha IELs derived from two distinct thymic precursors have staggered ontogeny. J Exp Med 217.

27. O'Reilly LA, Kruse EA, Puthalakath H, Kelly PN, Kaufmann T, Huang DC, and Strasser A. 2009. MEK/ERK-mediated phosphorylation of Bim is required to ensure survival of T and B lymphocytes during mitogenic stimulation. J Immunol 183: 261–269. [PubMed: 19542438]

28. Cheng EH, Wei MC, Weiler S, Flavell RA, Mak TW, Lindsten T, and Korsmeyer SJ. 2001. BCL-2, BCL-X(L) sequester BH3 domain-only molecules preventing BAX- and BAK-mediated mitochondrial apoptosis. Mol Cell 8: 705–711. [PubMed: 11583631]

29. Bouillet P, Purton JF, Godfrey DI, Zhang LC, Coultas L, Puthalakath H, Pellegrini M, Cory S, Adams JM, and Strasser A. 2002. BH3-only Bcl-2 family member Bim is required for apoptosis of autoreactive thymocytes. Nature 415: 922–926. [PubMed: 11859372]

30. Li KP, Fahnrich A, Roy E, Cuda CM, Grimes HL, Perlman HR, Kalies K, and Hildeman DA. 2017. Temporal Expression of Bim Limits the Development of Agonist-Selected Thymocytes and Skews Their TCRbeta Repertoire. J Immunol 198: 257–269. [PubMed: 27852740]

31. Wojciechowski S, Jordan MB, Zhu Y, White J, Zajac AJ, and Hildeman DA. 2006. Bim mediates apoptosis of CD127(lo) effector T cells and limits T cell memory. Eur J Immunol 36: 1694–1706. [PubMed: 16761315]

32. Wojciechowski S, Tripathi P, Bourdeau T, Acero L, Grimes HL, Katz JD, Finkelman FD, and Hildeman DA. 2007. Bim/Bcl-2 balance is critical for maintaining naive and memory T cell homeostasis. J Exp Med 204: 1665–1675. [PubMed: 17591857]

33. Kurtulus S, Tripathi P, Moreno-Fernandez ME, Sholl A, Katz JD, Grimes HL, and Hildeman DA. 2011. Bcl-2 allows effector and memory CD8+ T cells to tolerate higher expression of Bim. J Immunol 186: 5729–5737. [PubMed: 21451108]

34. Wirasinha RC, Chan A, Yap JY, Hu DY, Teh CE, Gray DHD, Goodnow CC, and Daley SR. 2019. Deletion of self-reactive CCR7– thymocytes in the absence of MHC expression on thymic epithelial cells. Cell Death Differ 26: 2727–2739. [PubMed: 31019259]

35. Pobezinsky LA, Angelov GS, Tai X, Jeurling S, Van Laethem F, Feigenbaum L, Park JH, and Singer A. 2012. Clonal deletion and the fate of autoreactive thymocytes that survive negative selection. Nat Immunol 13: 569–578. [PubMed: 22544394]

36. Lai YG, Hou MS, Lo A, Huang ST, Huang YW, Yang-Yen HF, and Liao NS. 2013. IL-15 modulates the balance between Bcl-2 and Bim via a Jak3/1-PI3K-Akt-ERK pathway to promote CD8alphaalpha+ intestinal intraepithelial lymphocyte survival. Eur J Immunol 43: 2305–2316. [PubMed: 23754237]

37. Nakayama K, Nakayama K, Negishi I, Kuida K, Sawa H, and Loh DY. 1994. Targeted disruption of Bcl-2 alpha beta in mice: occurrence of gray hair, polycystic kidney disease, and lymphocytopenia. Proc Natl Acad Sci U S A 91: 3700–3704. [PubMed: 8170972]

38. Raynor J, Sholl A, Plas DR, Bouillet P, Chougnet CA, and Hildeman DA. 2013. IL-15 Fosters Age-Driven Regulatory T Cell Accrual in the Face of Declining IL-2 Levels. Front Immunol 4: 161. [PubMed: 23805138]

39. Herold MJ, Stuchbery R, Merino D, Willson T, Strasser A, Hildeman D, and Bouillet P. 2014. Impact of conditional deletion of the pro-apoptotic BCL-2 family member BIM in mice. Cell Death Dis 5: e1446. [PubMed: 25299771]

40. Lefrancois L, and Lycke N. 2001. Isolation of mouse small intestinal intraepithelial lymphocytes, Peyer's patch, and lamina propria cells. Curr Protoc Immunol Chapter 3: Unit 3 19.

41. Thorp E, Li Y, Bao L, Yao PM, Kuriakose G, Rong J, Fisher EA, and Tabas I. 2009. Brief report: increased apoptosis in advanced atherosclerotic lesions of Apoe–/– mice lacking macrophage Bcl-2. Arterioscler Thromb Vasc Biol 29: 169–172. [PubMed: 18988889]

42. Kurd NS, Hoover A, Yoon J, Weist BM, Lutes L, Chan SW, and Robey EA. 2021. Factors that influence the thymic selection of CD8alphaalpha intraepithelial lymphocytes. Mucosal Immunol 14: 68–79. [PubMed: 32483197]

43. Guo X, Tanaka Y, and Kondo M. 2015. Thymic precursors of TCRalphabeta(+)CD8alphaalpha(+) intraepithelial lymphocytes are negative for CD103. Immunol Lett 163: 40–48. [PubMed: 25448708]

44. Sato T, Ohno S, Hayashi T, Sato C, Kohu K, Satake M, and Habu S. 2005. Dual functions of Runx proteins for reactivating CD8 and silencing CD4 at the commitment process into CD8 thymocytes. Immunity 22: 317–328. [PubMed: 15780989]

45. Moran AE, Holzapfel KL, Xing Y, Cunningham NR, Maltzman JS, Punt J, and Hogquist KA. 2011. T cell receptor signal strength in Treg and iNKT cell development demonstrated by a novel fluorescent reporter mouse. J Exp Med 208: 1279–1289. [PubMed: 21606508]

46. Akbar AN, Borthwick NJ, Wickremasinghe RG, Panayoitidis P, Pilling D, Bofill M, Krajewski S, Reed JC, and Salmon M. 1996. Interleukin-2 receptor common gamma-chain signaling cytokines regulate activated T cell apoptosis in response to growth factor withdrawal: selective induction of anti-apoptotic (bcl-2, bcl-xL) but not pro-apoptotic (bax, bcl-xS) gene expression. Eur J Immunol 26: 294–299. [PubMed: 8617294]

47. Zhu Y, Swanson BJ, Wang M, Hildeman DA, Schaefer BC, Liu X, Suzuki H, Mihara K, Kappler J, and Marrack P. 2004. Constitutive association of the proapoptotic protein Bim with Bcl-2-related proteins on mitochondria in T cells. Proc Natl Acad Sci U S A 101: 7681–7686. [PubMed: 15136728]

48. Chopp LB, Gopalan V, Ciucci T, Ruchinskas A, Rae Z, Lagarde M, Gao Y, Li C, Bosticardo M, Pala F, Livak F, Kelly MC, Hannenhalli S, and Bosselut R. 2020. An Integrated Epigenomic and Transcriptomic Map of Mouse and Human alphabeta T Cell Development. Immunity 53: 1182–1201 e1188. [PubMed: 33242395]

49. Oh-Hora M, Komatsu N, Pishyareh M, Feske S, Hori S, Taniguchi M, Rao A, and Takayanagi H. 2013. Agonist-selected T cell development requires strong T cell receptor signaling and store-operated calcium entry. Immunity 38: 881–895. [PubMed: 23499491]

50. Lauritsen JP, Kurella S, Lee SY, Lefebvre JM, Rhodes M, Alberola-Ila J, and Wiest DL. 2008. Egr2 is required for Bcl-2 induction during positive selection. J Immunol 181: 7778–7785. [PubMed: 19017967]

51. Lai YG, Hou MS, Hsu YW, Chang CL, Liou YH, Tsai MH, Lee F, and Liao NS. 2008. IL-15 does not affect IEL development in the thymus but regulates homeostasis of putative precursors and mature CD8 alpha alpha+ IELs in the intestine. J Immunol 180: 3757–3765. [PubMed: 18322181]

52. Lambolez F, Azogui O, Joret AM, Garcia C, von Boehmer H, Di Santo J, Ezine S, and Rocha B. 2002. Characterization of T cell differentiation in the murine gut. J Exp Med 195: 437–449. [PubMed: 11854357]

53. Konkel JE, Maruyama T, Carpenter AC, Xiong Y, Zamarron BF, Hall BE, Kulkarni AB, Zhang P, Bosselut R, and Chen W. 2011. Control of the development of CD8alphaalpha+ intestinal intraepithelial lymphocytes by TGF-beta. Nat Immunol 12: 312–319. [PubMed: 21297643]

54. McKean DJ, Huntoon CJ, Bell MP, Tai X, Sharrow S, Hedin KE, Conley A, and Singer A. 2001. Maturation versus death of developing double-positive thymocytes reflects competing effects on Bcl-2 expression and can be regulated by the intensity of CD28 costimulation. J Immunol 166: 3468–3475. [PubMed: 11207305]

55. Gray DH, Kupresanin F, Berzins SP, Herold MJ, O'Reilly LA, Bouillet P, and Strasser A. 2012. The BH3-only proteins Bim and Puma cooperate to impose deletional tolerance of organ-specific antigens. Immunity 37: 451–462. [PubMed: 22960223]

56. Erlacher M, Labi V, Manzl C, Bock G, Tzankov A, Hacker G, Michalak E, Strasser A, and Villunger A. 2006. Puma cooperates with Bim, the rate-limiting BH3-only protein in cell death during lymphocyte development, in apoptosis induction. J Exp Med 203: 2939–2951. [PubMed: 17178918]

57. Williams O, Norton T, Halligey M, Kioussis D, and Brady HJ. 1998. The action of Bax and bcl-2 on T cell selection. J Exp Med 188: 1125–1133. [PubMed: 9743531]

58. Reis BS, Hoytema van Konijnenburg DP, Grivennikov SI, and Mucida D. 2014. Transcription factor T-bet regulates intraepithelial lymphocyte functional maturation. Immunity 41: 244–256. [PubMed: 25148025]

59. Wirasinha RC, Singh M, Archer SK, Chan A, Harrison PF, Goodnow CC, and Daley SR. 2018. alphabeta T-cell receptors with a central CDR3 cysteine are enriched in CD8alphaalpha intraepithelial lymphocytes and their thymic precursors. Immunol Cell Biol 96: 553–561. [PubMed: 29726044]

60. Lutz C, Mozaffari M, Tosevski V, Caj M, Cippa P, McRae BL, Graff CL, Rogler G, Fried M, and Hausmann M. 2015. Increased lymphocyte apoptosis in mouse models of colitis upon ABT-737 treatment is dependent upon BIM expression. Clin Exp Immunol 181: 343–356. [PubMed: 25845418]

Key points:

Bcl-2 promotes survival of thymic precursors of TCRαβ+ CD8αα+ IEL by antagonizing Bim

CD122+ DN IELp that co-express Runx3 and α4β7 display the highest Bcl-2 dependence

Mice with thymic loss of Bcl-2 have an almost complete loss of gut TCRαβ+ CD8αα+ IEL
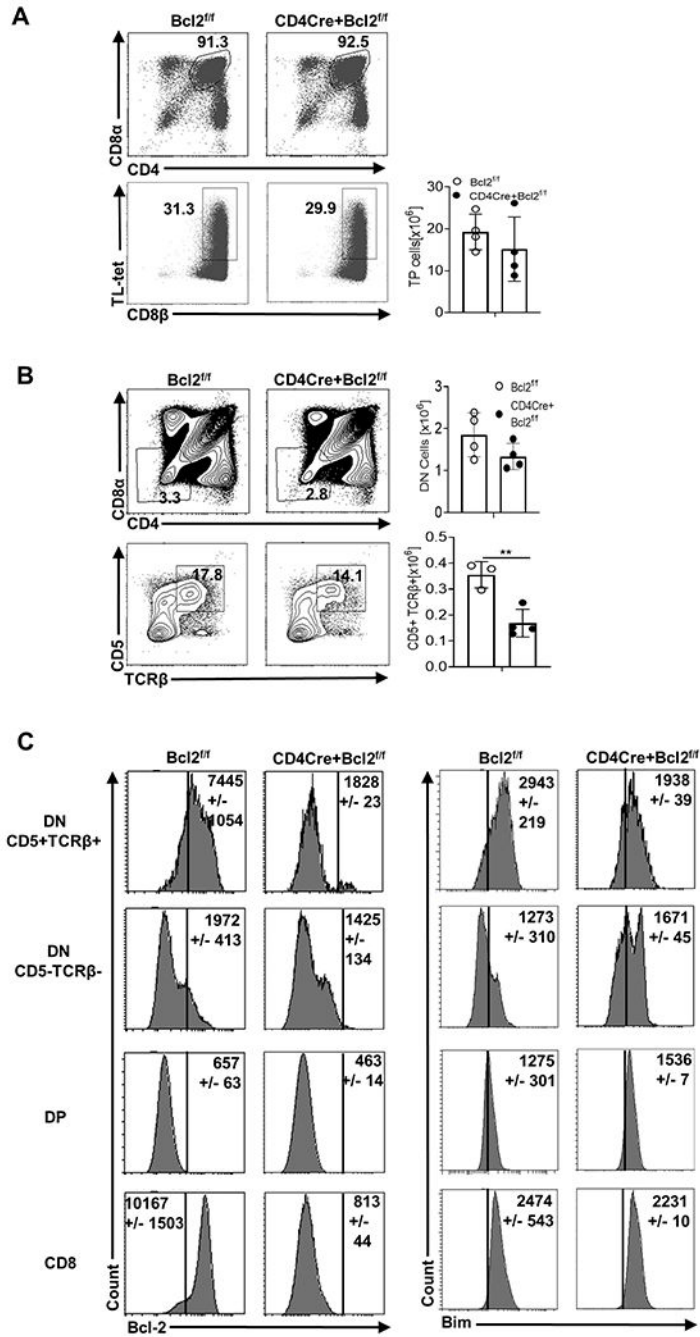
Fig 1. Bcl-2 contributes to the survival of CD5+ TCRβ+ DN thymocytes

(A) Within CD4+ CD8+ thymocytes, triple positive (CD4+ CD8αα+ CD8αβ+) pre-selection precursors of TCRαβ+ CD8αα+ IEL were identified by gating on Thymus Leukemia (TL) antigen tetramer positive cells and CD8β. (B) CD25− CD1dtet− CD4− CD8− DN (top row) and within the DN, post-selected CD5+ TCRβ+ thymocytes (bottom row) were determined. Numbers in representative plots show the percentage and bar graphs show the numbers of each population from Bcl2^f/f (open circle) and CD4CreBcl2^f/f (filled circle) mice. (C) Histograms show the mean fluorescence intensity(MFI)[11] of Bcl-2 and

Bim in CD5+ TCRβ+ DN, CD5− TCRβ− DN, DP and CD8+ thymocytes from Bcl2$^{f/f}$ and CD4CreBcl2$^{f/f}$ mice. Results are representative of at least three independent experiments with n=3 or more mice per group and show mean ± SD. **$p < 0.01$, Student's t test.

---

[11]MFI mean fluorescence intensity
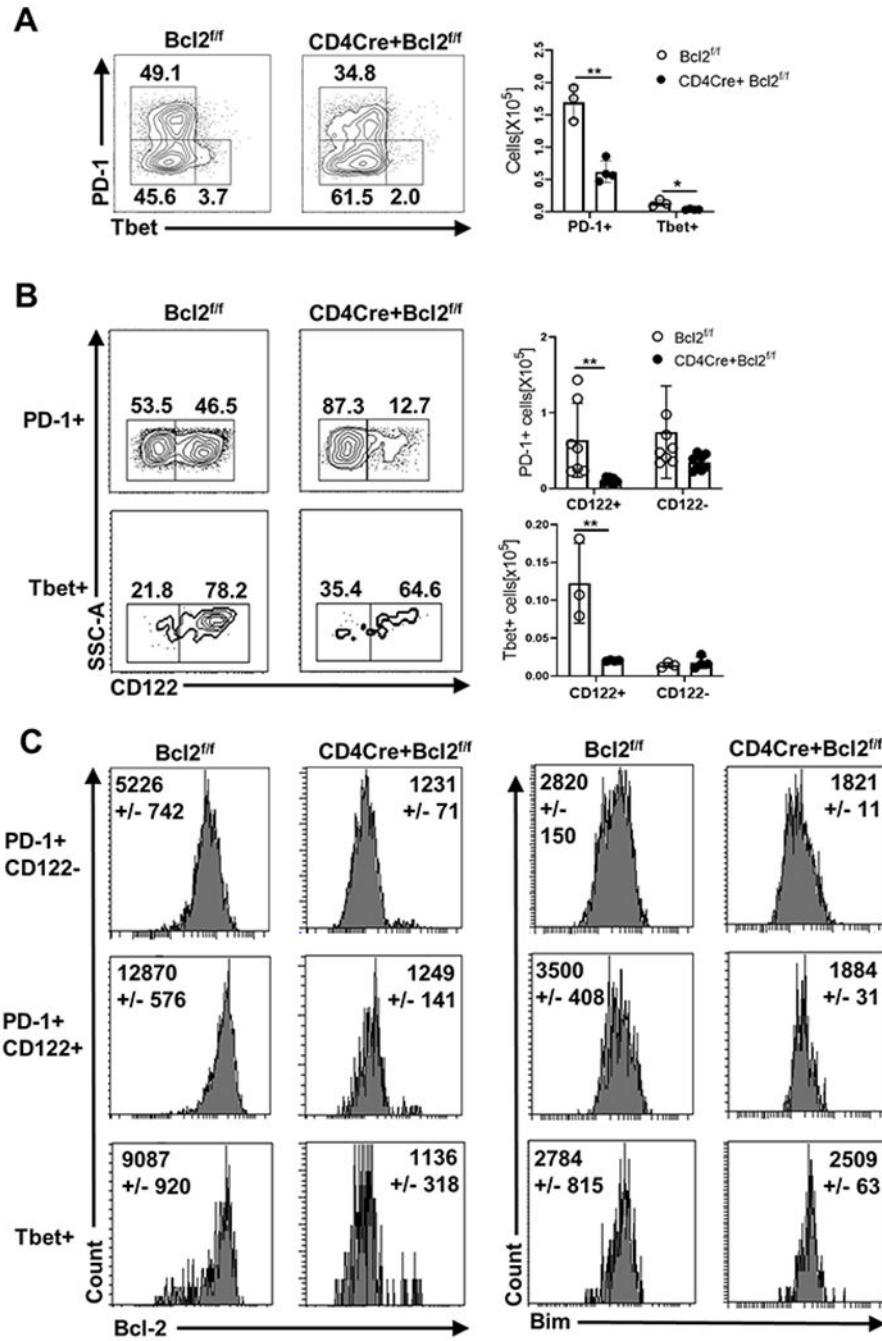
Fig 2. Bcl-2 is critical for the survival of CD122+ thymocytes

(A) Within CD5+ TCRβ+ DN thymocytes, PD-1 and Tbet expressing populations were identified. (B) Within the PD-1+ and Tbet+ cells, CD122 expressing populations were identified. Numbers in representative plots show the percentage and bar graphs show the numbers from Bcl2$^{f/f}$ (open circle) and CD4CreBcl2$^{f/f}$ (filled circle) mice. (C) Histograms show Bcl-2 and Bim expression in PD-1+ CD122−, PD-1+ CD122+ and Tbet+ populations in Bcl2$^{f/f}$ and CD4CreBcl2$^{f/f}$ mice. Results are representative of at least four independent

experiments with n=3 or more mice per group and show mean ± SD. **$p < 0.01$, Student's t test.
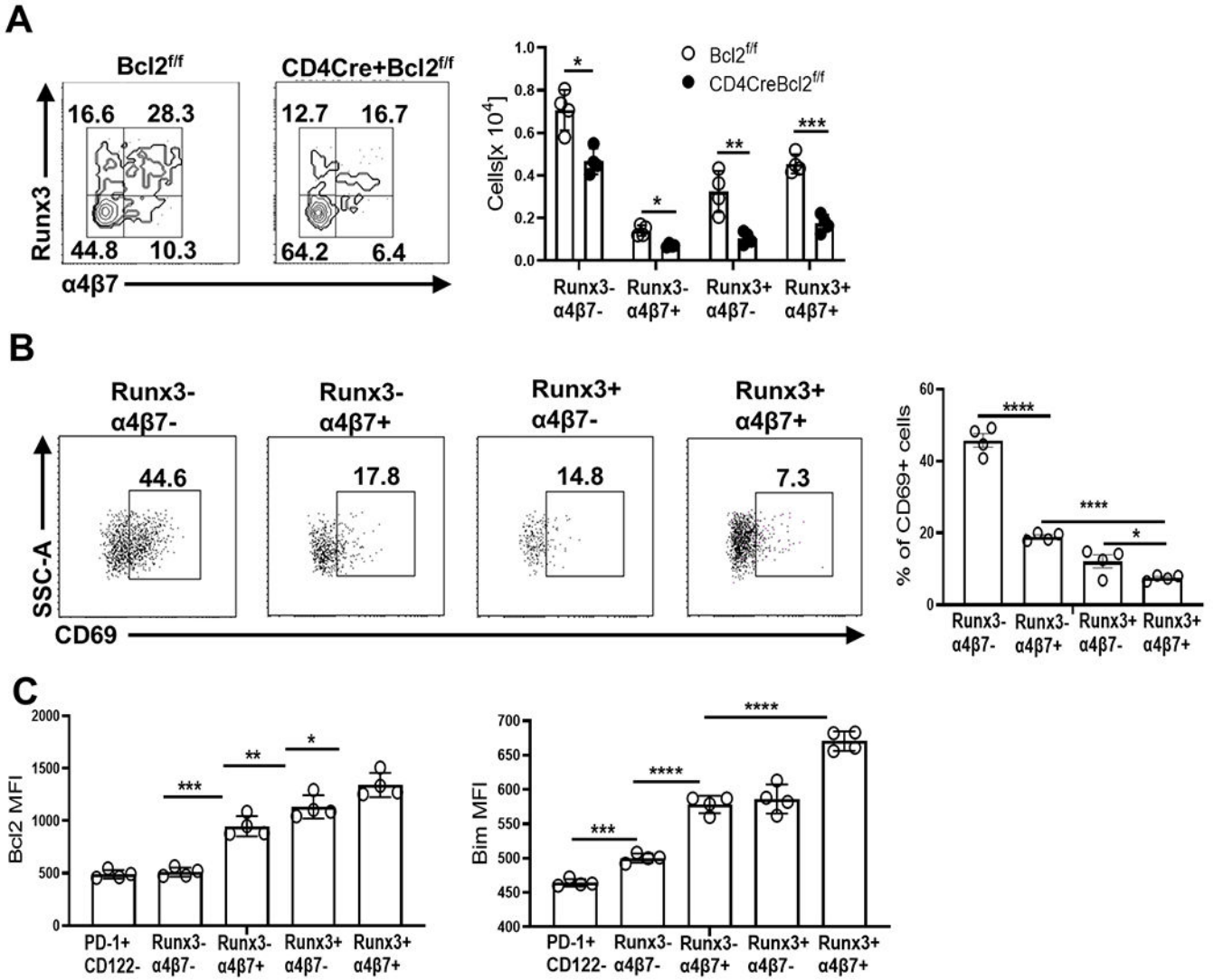
Fig 3. Runx3 expression marks a mature IELp sub-population among PD-1+ CD122+ thymocytes that critically depends on Bcl-2 for survival

(A) Flow cytometric identification of Runx3– α4β7– , Runx3– α4β7+, Runx3+ α4β7– and Runx3+ α4β7+ sub-populations within PD0-1+ CD122+ CD44^{lo} post-selected DN thymocytes. The bar graphs show the numbers of each population from Bcl2$^{f/f}$ (open circle) and CD4CreBcl2$^{f/f}$ (filled circle) mice. (B) Representative dot plots and bar graphs show the percentage of CD69+ cells among sub-populations of PD-1+ CD122+ CD44^{lo} thymocytes in WT mice (C) Bar graphs show the MFI of Bcl-2 and Bim in the sub-populations of PD-1+ CD122+CD44^{lo} thymocytes from WT mice in comparison to PD-1+ CD122– cells. Results are representative of 3 independent experiments with n=3 or more mice per group and show mean ± SD. *$p < 0.05$, **$p < 0.01$, ***$p < 0.001$, ***$p < 0.0001$ Student's t test.
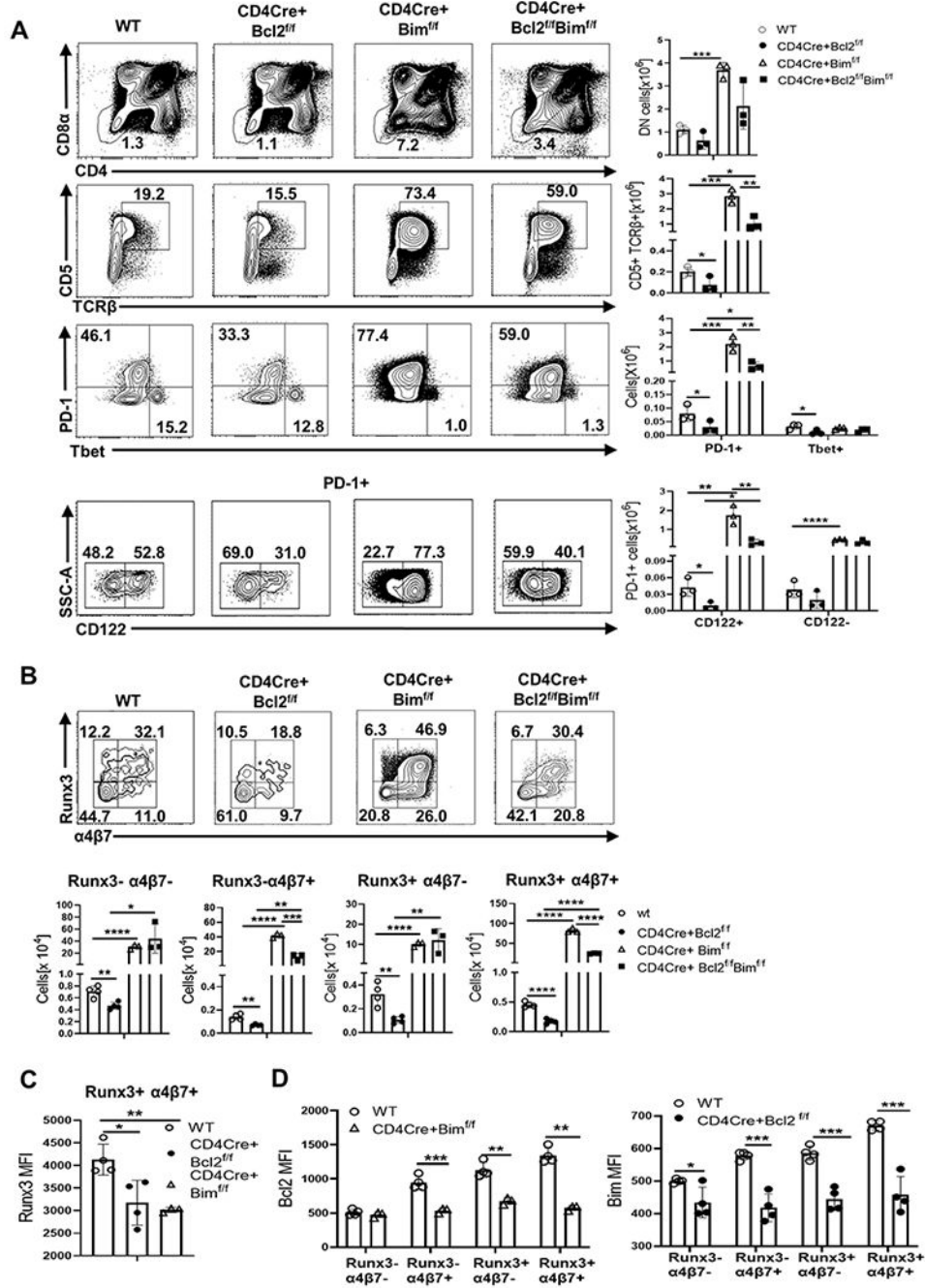
Fig 4. Bcl-2 antagonizes Bim to maintain survival of CD122+ IELp

Dot plots show frequencies and bar graphs show thymocyte numbers from WT (open circle), CD4Cre+Bcl2[f/f] (filled circle), and CD4CreBim[f/f] (open triangle) and CD4CreBim[f/f] Bcl2[f/f] (filled square) mice of (A) DN (CD25– CD1tet– CD4– CD8–) (Row 1) , CD5+ TCRβ+ among DN (Row 2), PD-1+ and Tbet+ among CD5+ TCRβ+ DN (Row 3) , and CD122+ and CD122– among the PD-1+ (Row 4) (B) Runx3– α4β7– , Runx3– α4β7+ , Runx3+ α4β7– and Runx3+ α4β7+ cells within PD-1+ CD122+ CD44^{lo} thymocytes (C) Bar graph compares MFI of Runx3 in the Runx3+ α4β7+ sub-population in WT (open circle),

CD4CreBcl2$^{f/f}$ (filled circle), and CD4CreBim$^{f/f}$ (open triangle) mice. (D) Bar graphs compare MFI of Bcl-2 in Runx3− α4β7− , Runx3− α4β7+ , Runx3+ α4β7− and Runx3+ α4β7+ sub-populations between WT (open circle) and CD4CreBim$^{f/f}$ (filled square) mice and of Bim between WT (open circle) and CD4CreBcl2$^{f/f}$ (filled circle) mice. Results are representative of at least 3 independent experiments with n=3 or more mice per group and show mean ± SD. *$p < 0.05$, **$p < 0.01$, ***$p < 0.001$, **** $p < 0.0001$ Student's t test.
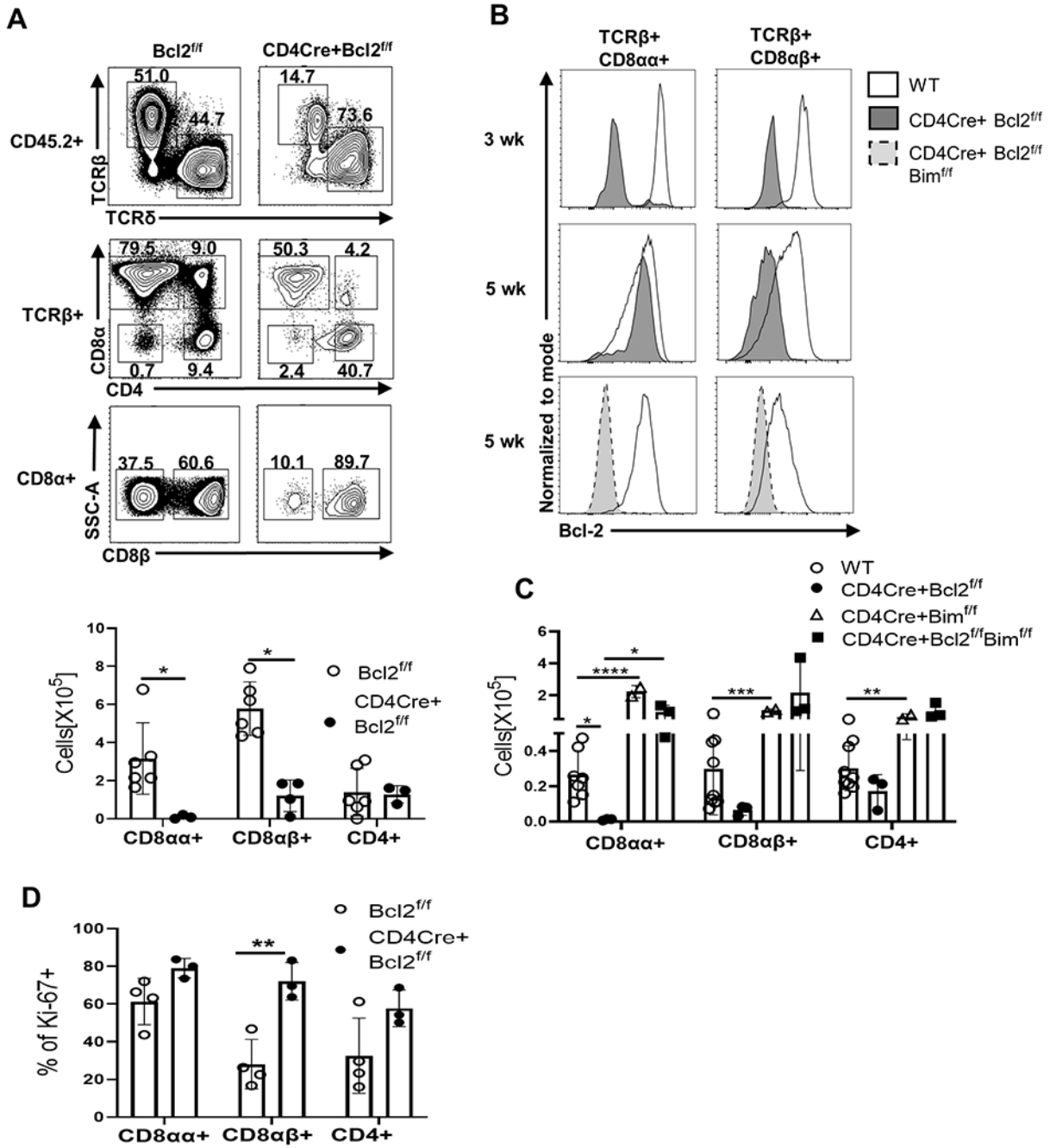
Fig 5. Thymic deletion of Bcl-2 leads to a profound loss of TCRαβ+ CD8αα+ IEL
(A)Representative dot plots indicate frequency of gut IEL populations (gated from live, CD45.2+ cells) and show TCRβ+ and TCRδ+ IEL(top row), CD8α and CD4 expression among TCRβ+ IEL(middle row) and CD8β expression among the CD8α+ IEL (bottom row) .The bar graph shows the numbers of TCRαβ+ CD8αα+, TCRαβ+ CD8αβ+ and TCRαβ+ CD4+ IEL from 8 week old Bcl2^{f/f} (open circle) and CD4CreBcl2^{f/f} (filled circle) mice. (B) Histograms show Bcl-2 expression in TCRαβ+ CD8αα+ IEL (left column) and TCRαβ+ CD8αβ+ IEL (right column) from 3 week old and 5 week old WT (solid

no fill) and CD4CreBcl2$^{f/f}$ (solid grey fill) mice and 5 week old WT (solid no fill) and CD4CreBcl2$^{f/f}$ Bim$^{f/f}$ (dashed light grey fill) mice. (C) Bar graphs show numbers of IEL in WT (open circle) and CD4CreBcl2$^{f/f}$ (filled circle) at 3 weeks of age and CD4CreBim$^{f/f}$ (open triangle) and CD4CreBim$^{f/f}$ Bcl2$^{f/f}$ (filled square) at 5 weeks of age. D) Bar graph shows the frequency of Ki-(A) 67+ cells among TCRαβ+ CD8αα+, TCRαβ+ CD8αβ+ and TCRαβ+ CD4+ IEL from 3 week old Bcl2$^{f/f}$ mice (open circles) and CD4Cre+Bcl2$^{f/f}$ mice (filled circles). Results are representative of at least 3 independent experiments with n=3 or more mice per group and show mean ± SD. *$p < 0.05$, **$p < 0.01$, ***$p < 0.001$, **** $p < 0.0001$ Student's t test.